Preprint of: Arshaghi A., Razmjooy N., Estrela V. V., Burdziakowski P., Nascimento D. A., Deshpande A., Patavardhan P.P., Image transmission in UAV MIMO UWB-OSTBC system over Rayleigh channel using multiple description coding (MDC), In: Estrela V. V., Hemanth J., Saotome O., Nikolakopoulos G., Sabatini R. (ed.): 'Imaging and Sensing for Unmanned Aircraft Systems: Volume 2: Deployment and Applications' (Control, Robotics & Sensors, 2020) DOI: 10.1049/PBCE120G IET Digital Library, https://digital-library.theiet.org/content/books/ce/pbce120g

Image Transmission in UAV MIMO UWB-OSTBC System over Rayleigh Channel Using Multiple Description Coding (MDC)

Ali Arshaghi1, Navid Razmjooy2, Vania V. Estrela3, Pawel Burdziakowski4, Douglas A. Nascimento5, Anand Deshpande6, Prashant P. Patavardhan7

1Department of Electrical Engineering, Central Tehran Branch, Islamic Azad University, Tehran, Iran
ali.arshaghi@gmail.com ,
2Department of Electrical Engineering, Tafresh University, Tafresh, Iran
xnavid@gmail.com
3 Telecommunications Department, Federal Fluminense University (UFF), Rio de Janeiro, Brazil
vania.estrela.phd@ieee.org
4Faculty of Civil and Environmental Engineering, Gdansk University of Technology, Poland
pawelburdziakowski@gmail.com
5 Department of Electrical and Computer Engineering, Texas A&M University at Qatar, Doha, Qatar
eng.douglas.a@ieee.org
6 Department of Electronics and Communication Engineering, Angadi Institute of Technonoly and Management Belagavi, Karnataka, India
deshpande.anandb@gmail.com
7 Department of Electronics and Communication Engineering, Gogte Institute of Technology, Belagavi, Karnataka, India
pppatavardhan@git.edu

Abstract- Orthogonal Space-Time Block Codes (OSTBC) and multiple-input-multiple-output (MIMO) communication system are new techniques with high performance that have many applications in wireless telecommunications. This chapter presents an image transfer technique for the unmanned aerial vehicle (UAV) in a UWB system using a hybrid structure of the MIMO-OSTBC wireless environment in Multiple Description Coding (MDC) deals. MDC technique for image transmission is a new approach in which there is no record of it so far. This ensures that in the packet loss scenario due to channel errors, images with acceptable quality with no need for retransmission can be reconstructed. The proposed system is implemented using a different number of transmitter and receiver antennas UAV. Assuming a Rayleigh model for the communication channels, the MDC image transmission performance is compared with single description coding (SDC). Experimental results confirm that the proposed hybrid method has better performance than the single description coding.

Keywords: Image transmission, UAV, UWB, Orthogonal Space-Time Block Code, OSTBC, MIMO, Multiple Description Coding, MDC, SDC, Alamouti coding

I. INTRODUCTION

The unmanned aerial vehicle (UAV) technology has a lot of potential such that they are remarkably increasing especially in recent years. Some of these applications include filming, entertainment, accident relief, building management agriculture, and commercial UAV cargo carrying. The application of this technology is expected to increase from 80,000 units in 2015 to 2.7 million units in 2025, and the big

companies are looking to use UAVs in rural areas [1].

UAV can also be used to deliver a broadband wireless connection to hot spot areas in transit times during emergencies and disasters such as earthquakes when the communications infrastructure may be damaged [2].

This interest in UAVs leads individuals towards studying aeroplane gaming (AG) with augmented reality (AR), UAV channels for the link budget analysis, and the UAV cyber-physical systems' (CPSs) design [70, 71, 72]. In the end, UWB signals are allowed to receive multipath components (MPCs) with an outstanding temporary resolution, which may be a fascinating technology for the development of a broadband release model (UWB) [3-5].

The high bandwidth of the UWB can also facilitate high data rates, better penetration through materials, and coexistence with narrowband networks for air-to-ground (AG) UAV communications.

The UAV comprises a radio control and self-control program [6]. These UAVs usually use photovoltaic energy to transmit the information (like video and multimodal imagery) into a ground control station, called High-Definition Image Transmission System (HDIT), which plays an essential role in HD image processing and computer vision (CV) applications, including encoding, transferring, receiving, and decoding.

In particular, the application that transmits HD image and video data to a control office is a critical factor in controlling and directing the flight, so it requires a real-time performance.

In the field of optical measurements, aerial surveys, and air photography, high-resolution images are increasingly used in UAVs to improve the accuracy of observation to make the amount of the data extremely high.

The 1080p HD standard video (HDTV) standard produces approximately 500Mb of data per second at 3 frames per second with 8 bit YCbCr. The 2K, the 4K video format, is also used imperceptible as the next generation HD format, and it generates a large amount of data.

In most applications scenarios, the UAV requires aerial imagery components to be checked, and aerial photography can be real-time transmitted to the ground station. It is necessary to compress the images to control the data rate so that the bandwidth is low in the current UAV areas.

In addition, the UAV requires photovoltaic components to provide fast-moving characteristics. It is also very rigid in the power dissipation, volume and weight of the image transmission system [7].

Most traditional military aircraft uses data-linking technology to create a wireless communication system with studies suggesting it as a new scheme for sending a small UAV image.

The application areas of this chapter are extended from civilian airlift and aerial photography, resource exploration, power cable discovery, oil pipe monitoring, consumer vehicle, and video transmission of UAVs.

Compact video plays a real role in the implementation and operation of the system. Due to the growth of the techniques and the complexity of the system from the construction aspect, the technical implementation capability of this research carries the image transfer to the UAV with UWB and faces all the requirements including power dissipation, volume and weight.

H.264/AVC is the standard video encoder for the streaming, but the HEVC is becoming common. That coding framework and key technologies have been thoroughly analysed.

Often, the research and use of UAV-CPSs are limited to external experiments using global satellite navigation system (GNSS) receivers for guidance [8]. A visual observation control has recently been inspired by extensive aerial robotic research that has been inspired by the complexity and the precision of the aerial manoeuvres [9].

The low cost and high-speed progression make the UAVs to be useful in the internal applications in the emergencies [10]. The advancement in UWB communication offers a high positioning accuracy that provides a new range of applications [11].

The concept of ultra-wide bandwidth spread-spectrum impulse radio has been discussed in [12] as an alternative for communication of short suffering. The ability to solve the multi-path playback makes it a viable candidate for internal locating [13].

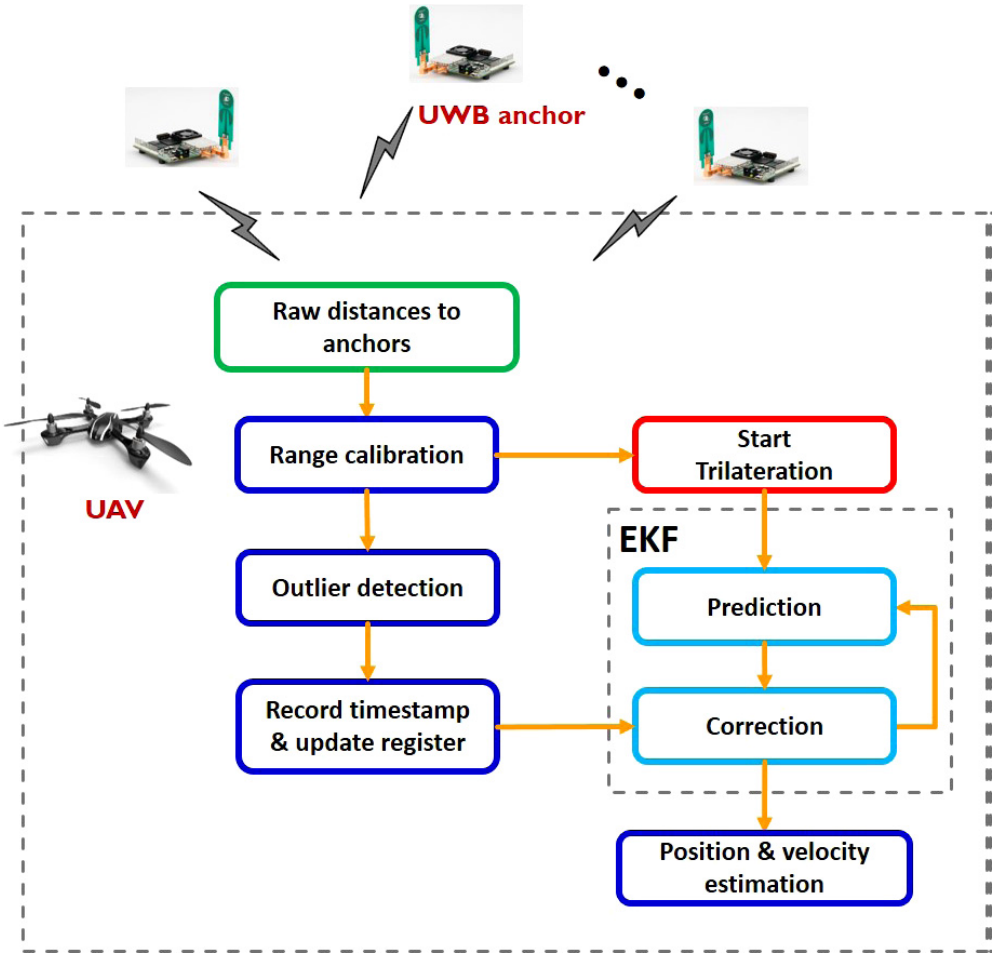

Fig. 1. UWB-based localisation workflow.

The micro UAV technology (MAV) has a lot of potential usages in recent years. Moreover, UAV air photography can also be used in 3D mapping [14], airborne surveying [15], agricultural precision [16], as well as search and rescue [17], and other interesting applications [18].

The method of work for the UWB centralisation system appears in Fig. (1). In [19], UWB radios are used to estimate the location and the speed of a quadcopter.

The UWB module on the quadcopter for distance measurement is to send ranging requests to anchor nodes.

In [20], low-cost high-accuracy UWB radios for internal localisation are proposed, which allows tracking drones in and out a warehouse for possible autonomous inventory taking.

The designed method is an Ultra-Wideband (UWB) solution that uses anchor nodes structure. So, it does not need any wired backbones and the battery will stay strong.

We developed a UWB MAC multi-technology protocol for localisation that does not need to be built-

in, such as Wi-Fi or Ethernet. In Fig. (2), the top-level system diagram of the proposed solution is drawn.

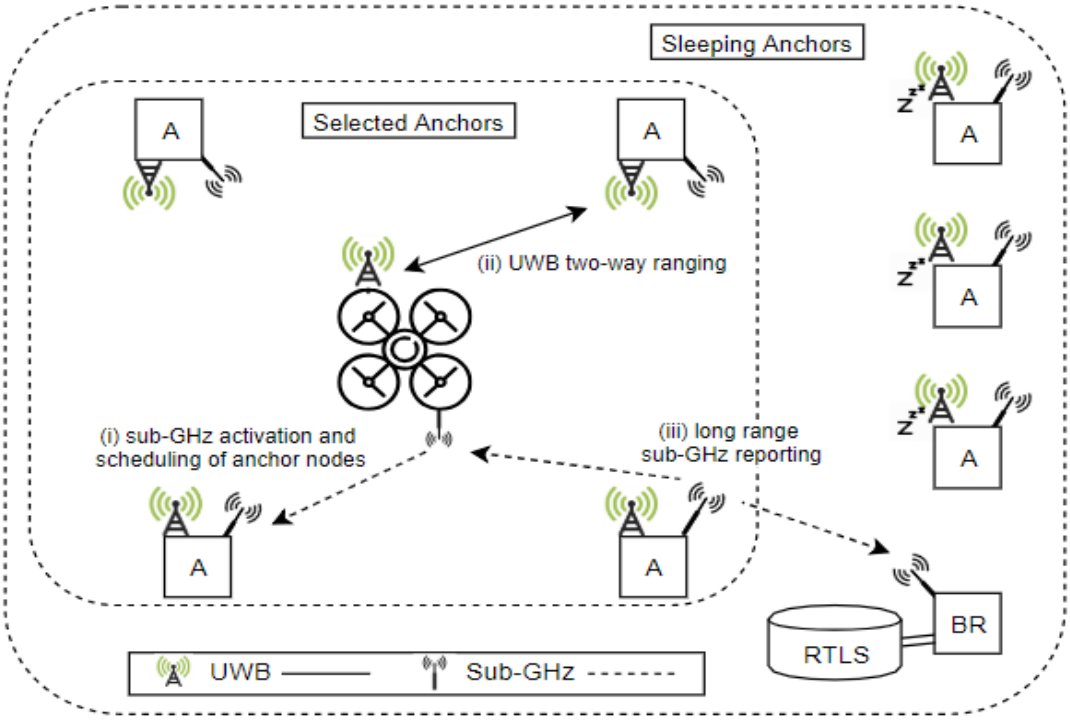

Fig. 2. High-level of the UWB localisation system with battery powered anchor nodes.

Image transmission owns a large volume of data and various value information bits than data transmission [21, 22]. Wireless communication high-dimensional image and video transmission have much application such as biomedical wireless sensor network, mobile networks, satellite networks, wireless sensor networks, and contingency [22-26]. Since multimedia wireless communication has played a paramount role in the communication field in recent years, the wireless image transmission is widely used. Many technologies have been proposed to improve the performance of image transmission system to get better image quality[27, 76, 77].

One of the systems for image transmission is the UWB, which is suitable for the transmission of high-dimensional high-resolution multimodal imageries. UWB communication system is a new technique with high performance that has low power consumption and many applications of wireless telecommunications for ultra-data rates. UWB affords an appropriate solution for telecommunication wireless high-speed with short-range. The radio technology can use 25% of the bandwidth of the centre frequency. Power UWB system is low in-band frequency; because it can play in a wide frequency band. This system is robust

toward the distortion and the interference and has high contrast and high time resolution in the receiver.

Low complexity and low cost are some crucial advantages of the technology that expedite its deployment in mobile applications. In these systems, instead of sinusoidal carriers, very narrow pulses are transmitted, and system bandwidth will appear into many GHz [28]. The Time-Hopping UWB (TH-UWB) technique and the direct sequence ultra-wideband (DS-UWB) methods are the most popular UWB approaches.

So far, time-hopping (TH) methods relying on the Pulse Position Modulation (PPM) known as TH-UWB and employing direct sequence method by antipodal modulation (DS-UWB) have been built for image transmission of UWB systems [27, 29].

There are several types of researches about comparing in the AWGN channel; the performance of the modulation UWB in these systems is different. Researchers showed that the DS-UWB systems with antipodal modulation have better performance and lower complexity toward PPM [30, 31].

Orthogonal STBCs represent reputable and straight transmission patterns, which can tackle the same diversity order as the classical maximal-ratio combining. Since their original inventions by *Alamouti* in [32] and the generalisation by Tarokh *et al.* in[33], they used it in the MIMO communication systems. STBCs do the Maximum-Likelihood (ML) decoding and can be performed at the receiver, but the MIMO channel can be transformed into an equivalent scalar Gaussian channel with a response equal to the Frobenius norm of the channel matrix [34, 35]. Some theoretical modelling and simulations [36, 37] though, have explained that the Nakagami-m distribution [38] and other situation is *Rayleigh/Ricean* distributions. The majority of related studies used the Rayleigh or Ricean fading statistics model [39, 40].

A MIMO system has more bandwidth application for the broadband and achieves more data rates by using the MIMO antennas. To achieve more data rates of 1 Gb/s in wireless telecommunications, one can use the system combination of the UWB and MIMO technologies [41].

A. The Efficiency of the Flat Rayleigh Fading Channel

The symbol error probability for a frequency-nonselective Rayleigh fading channel in QPSK ($M = 4$) can be presented as follows [42]:

$$p_s^{QPSK} = \frac{3}{4} - \frac{1}{\pi}\sqrt{\frac{E_s/N_0}{2+E_s/N_0}}.\cot^{-1}\left(-\sqrt{\frac{E_s/N_0}{2+E_s/N_0}}\right) \tag{1}$$

The Multiple Description Coding (MDC) technique is suitable for wireless environments by assuming the risk of losing data. These techniques are used to improve the protection of image transmission and to

resist the corruption of data transmitted over wireless channels [43].

This chapter investigates the transmission of MDC images on OSTBC MIMO channels with QPSK modulation. Transmission of MDC images in the MIMO system is new research that with attention to a study conducted already has not been performed. This chapter evaluates the overall success rate of the proposed wireless Rayleigh channel to compare the achieved results with the results of [44]. The influence of each block is studied by changing the simulated blocks and their valid parameters. The achieved results of the method of MDC and single description coding SDC are compared with each other.

The chapter is structured as follows. Section 2 goes over the image MDC, along with its implementation. Then, the subsequent Section describes the MIMO system. Section 4 and Section 5 investigate, Diversity and ST coding, respectively. Section 6 presents the results of several simulations with different sets of t parameters changed to influence the implementation of the ideas this article proposes. To close, Section 7 presents and discusses the conclusions and ideas for future works.

II. MULTIPLE DESCRIPTION CODING (MDC)

MDC is a technique based on source code that protects the image quality against the errors of the channel. The main idea in MDC is to subsample the original image into 4 sub-images. Fig. (3) illustrates this procedure where each subsampled image has its pixels representation by a given colour and shape as follows: red circle pixels correspond to Image Version (IV) 1, blue square pixels form IV 2, the yellow diamond-shaped pixels form IV 3, and green stars-shape pixels form IV 4.

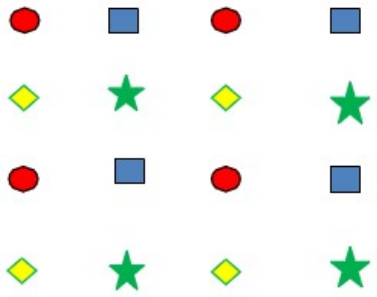

Fig. 3. Polyphase subsampling in the space domain image

For the sake of testing and validating the proposed system, the 256 × 256 Cameraman image is subsampled, thus resulting in 128 × 128 low-resolution pictures that will feed the MDC simulation like in Fig. (4)

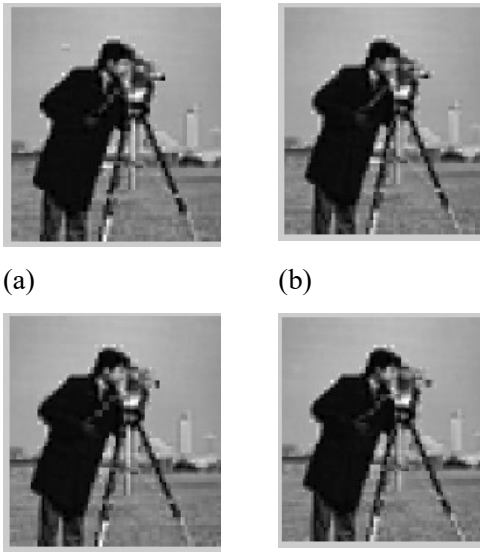

(a) (b)

(c) (d)

Fig. 4. Sub-images created in the transmitter

Each version is divided into 4 × 4 blocks. After that, the DCT transform of each block is calculated with the DC coefficient, and the next two AC coefficients of the blocks can be mapped to a vector. Hence, this vector feeds procedures corresponding to quantisation, source coding, channel coding, spreading and modulation to send signals thru the channel. In the UAV receiver part, the operation will do reversely. Fig. (5) depicts a block diagram of the overall four-stage framework is presented. According to Fig. (4), the original input image is divided into two or more versions of data (sub-images) [45].

Each version has a satisfactory quality of the original image. If all copies have been received by the UAV receiver, then the decoder reconstructed image data in high quality. Otherwise, the channel decoder will have low quality.

Decoders show the obtained subsampled image copies. Decoder 1234, for example, indicates that all four versions 1,2,3,4 have been received, and the rest of decoders presents the version numbers. Decode a string of input symbols $\{X_k\}_{\mathrm{k}=1}^{N}$ is transmitted through the four channels, $\{X_{ik}\}_{\mathrm{k}=1}^{N}$ is the string corresponding to *i*-th the decoder.

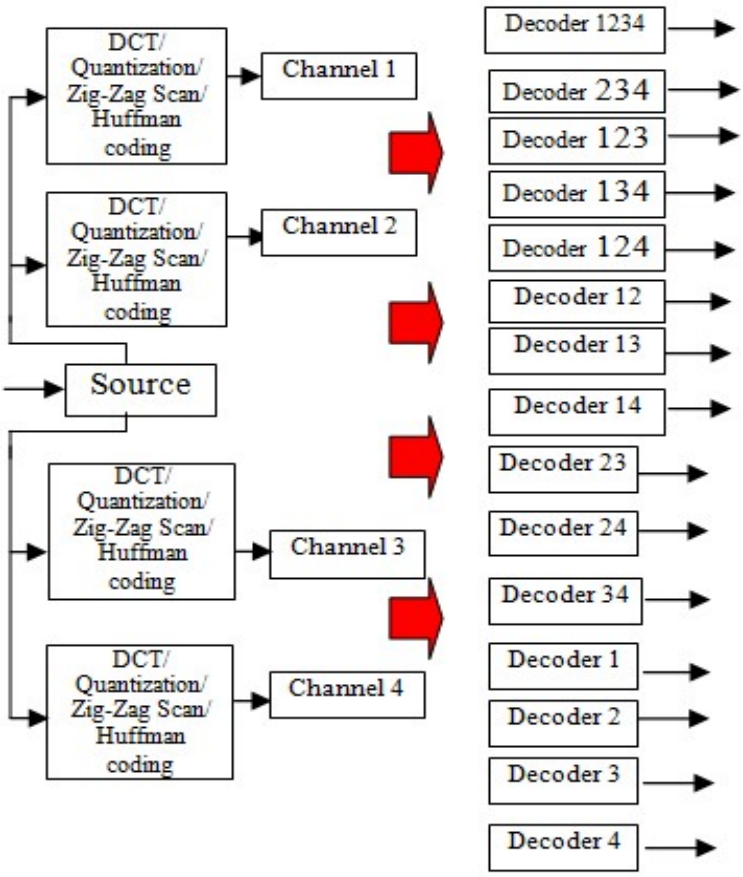

Fig. 5. The structure of four versions of the coding system based on the DCT

In this system, a total of 15 different scenarios are possible depending on the IV versions available at the UAV receiver for image reconstruction. Here, Decoder 1234 indicates that all four IVs have been received; Decoder 124 points to the reception of the IVs 1, 2 and 4; Decoder 34 signposts that IVs 3 and 4 have been received; and, finally, Decoder1 stands for the reception of the only IV1 only [45].

III. MIMO

Using techniques like MIMO antennas and OFDM helps to bring the most out of the 50 Mb/s data rates. As recommended in the IEEE802.11n, to reach the target of 1 Gb/s, more advanced techniques should be used. The UWB technology combined with MIMO might provide a solution. If $NT = NR = 1$, it is called a *single-input, single-output (SISO) system* and the corresponding channel is a *SISO channel*. The output of a frequency-selective SISO channel can be described by

$$y\,[k] = \sum_{k=0}^{L_t-1} h[K,k].x\,[K-k] + n\,[K] \tag{2}$$

MIMO system is, NI signals $x\mu[k]$, $1 \le \mu \le N$I, form the input at each time instant k and NO output signals $yv\,[k]$,

$1 \le v \le NO$ that pair (μ, v) of inputs and outputs is adjoined by a channel impulse response $hv[.], \mu[k, \kappa]$ [42]. Fig. (6) illustrates the structure of the MIMO system.

$$y_v[k] = \sum_{\mu=1}^{N_1} \sum_{k=0}^{L_t - 1} h_{v,k}[K,k] x_\mu[K-k] + n_v[K] \tag{3}$$

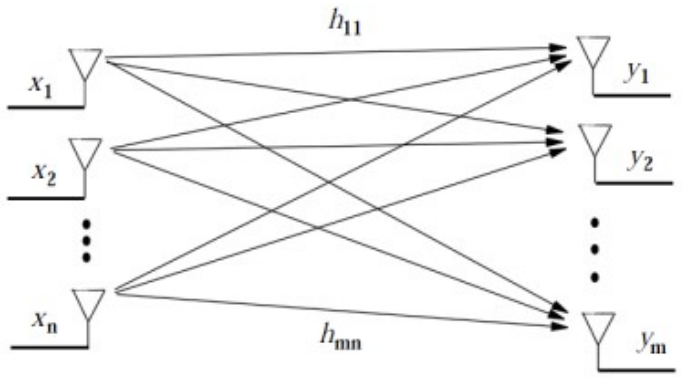

Fig. 6. MIMO system

The subsequent discrete-time model representing this system is

$$\begin{bmatrix} y_1 \\ \bullet \\ \bullet \\ \bullet \\ y_m \end{bmatrix} = \begin{bmatrix} h_{11} & \bullet & \bullet & \bullet & h_{1n} \\ \bullet & \bullet & & & \bullet \\ \bullet & & \bullet & & \bullet \\ \bullet & & & \bullet & \bullet \\ h_{m1} & \bullet & \bullet & \bullet & h_{mn} \end{bmatrix} \begin{bmatrix} x1 \\ \bullet \\ \bullet \\ \bullet \\ x_n \end{bmatrix} + \begin{bmatrix} N1 \\ \bullet \\ \bullet \\ \bullet \\ N_m \end{bmatrix} \tag{4}$$

$$\bar{y} = H\bar{x} + \bar{N} \tag{5}$$

where $\bar{x}$ is the n-dimensional vector with the transmitted symbols, $\bar{N}$ is the m-dimensional Additive White Gaussian Noise (AWGN) vector, $\boldsymbol{H}$ is a matrix that contains zero-mean complex circular Gaussian random variables, and h_{ij} represents the (gain) channel from the transmitting antenna j to the receiving antenna i [46]. Fig. (7) shows the general structure of the MIMO channel.

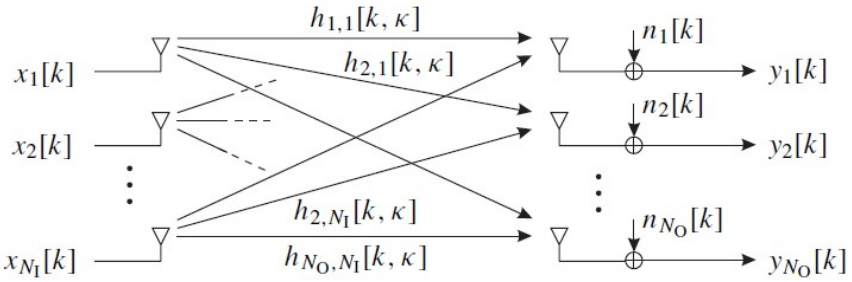

Fig. 7 The general structure of a frequency-selective MIMO channel

IV. DIVERSITY

MIMO systems afford diversity. Since there is a fading coefficient error in the mean value of the Signal-to-Noise-Ratio (SNR), AWGN channels have been improved a lot. The use of spatial diversity embraces methods to deal with the destructive effects of the channel. Composition spatial diversity with a type of diversity such as time or frequency can dramatically improve system performance. time-space codes simultaneously make the degree of diversity in time and space.

The spatial diversity systems use the multiple receive and transmit antenna arrays. The diversity gain represents the system reliability where the diversity gain states in the below equation reproduce the error rate evolution against the SNR [47].

$$d = -\lim_{SNR\to\infty} \frac{\log\left(p_e\left(SNR\right)\right)}{\log\left(SNR\right)} \tag{6}$$

where *Pe* (SNR) stands for the measured error rate at a fixed SNR value. one must use the *NT* transmitting antennas, and *NR* receiving antenna to acquire a maximum diversity gain of $NT \times NR$ in a MIMO system

In the MIMO systems, the Orthogonal Space-Time Block Code (OSTBC) encoder has been used for encoding an input symbol sequence. OSTBC mixes the input signal (from all of the receiving antennas), and the channel estimates the signal to extract the soft information about the OSTBC encoded symbols.

The MSE and the Peak Signal-to-Noise-Ratio (PSNR) are metrics to appraise the quality of the reconstructed image (after processing) given as a result of the following equations:

$$MSE = \frac{1}{M*N} \Sigma_{M,N} \left[I1(m,n) - I2(m,n) \right]^2 \tag{7}$$

$$PSNR = 10\log_{10}\frac{255^2}{MSE} \tag{8}$$

where, the previous expression assumes 256 grey levels, *M* and *N* correspond to a maximum number of rows and columns in the image respectively, *MSE* presents the cumulative Mean Squared Error between the reconstructed ($\boldsymbol{I_2}$) and the original ($\boldsymbol{I_1}$) images. The less value of the *MSE,* the less error on the image while the *PSNR* is increased.

V. SIMULATIONS RESULTS

This simulation illustrates all the proposed system rationale with the images the UAV sends and receives, along with the steps for sending and receiving information on the basic communications systems in this UAV system are also used to transfer images, run tasks sequentially for the channel coding modulation steps, and its opposite steps are taken to get the final image.

The block diagram for the proposed OSTBC-MIMO system for a UAV appears in Fig. (8). The MDC block acquires the 256 × 256 Cameraman frame and then, 128 × 128 subsampling process is applied to it. DCT is then used to the subsampled versions to quantise them into the next block to use an arithmetic code that is a source coding and at the next block using the convolutional channel coding.

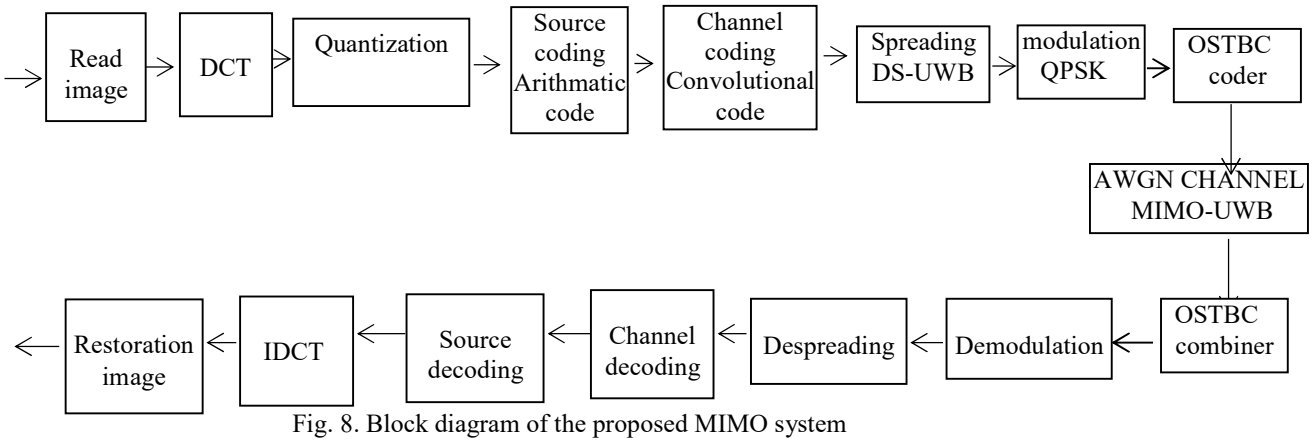

Fig. 8. Block diagram of the proposed MIMO system

Using of QPSK modulation, the channel is assumed to follow a Rayleigh distribution MIMO and gets the number of 2 × 2 and 2 × 1 antennas with 15dB SNR. In the UAV receiver, the reverse of the performed operations corresponding to decoding happens. In the next step of the UAV receiver, demodulation and channel decoding and source decoding following by IDCT are applied to the signals. After combining received sub-images with 128 × 128 dimensions, they are restored with 256 × 256 dimensions. The final received versions of the image in the UAV receiver appear in Fig. (9).

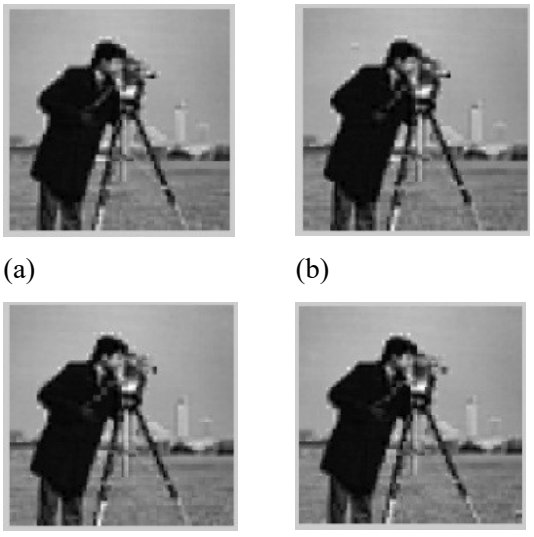
(a) (b)

(c) (d)

Fig. 9. Sub-images obtained in the receiver

The next Section illustrates how the mutual antenna coupling affects the performance of an OSTBC transmission over a MIMO channel. The simulation of the QPSK modulated Alamouti code for each SNR value with and without antenna coupling is shown in fig. (10). A realisation of the Alamouti code appears through the MIMO channel in each iteration.

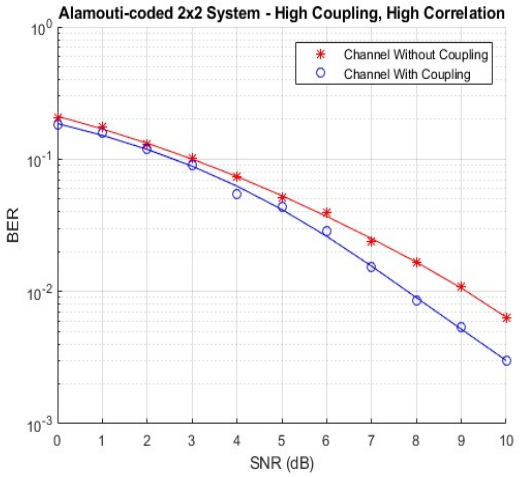

Fig. 10. The BER vs SNR curves plotted under different correlation and coupling scenarios

The 128 ×128 sub-sampled images are then combined to reconstruct the 256×256 original image with 15dB SNR (Fig. (11)).

Fig. 11. Image after the composition of the sub-image via QPSK

Average PSNR values for different number of lost versions using MDC with DCT transforms are given in Table 1. In cases where a prescription is lost, approximations copies of the missing parts can be recovered by averaging the matching pixels.

Table 1. PSNR vs different lost images scenarios

Number of Copies Lost	PSNR SNR=15dB
0	24.2543
1	23.0673
2	23.6530
3	22.2139

In Table 2, the PSNR of the received image for one state is illustrated only for DC coefficients of the original version. The PSNR of the reconstructed image based on the number of lost copies have been analysed in this case.

TABLE 2. PSNR DC COEFFICIENT IMAGES

Number of copies lost	PSNR SNR=15dB
0	20.5103
1	20.4975
2	20.4538
3	20.3125

Looking at the PSNR, one can attest that the image with 3 coefficients of DC, and AC copies has better quality toward the version that has just DC coefficient that PSNR 3 coefficients of DC and AC copies; because of using the 3 coefficient of the original image. Fig. (12) shows the PSNR values for the number of lost copies.

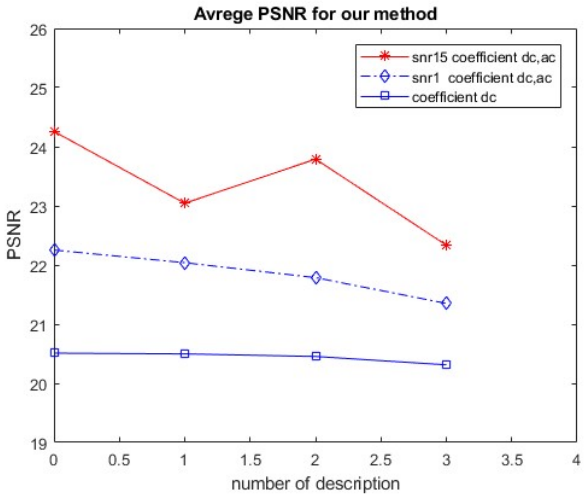

Fig. 12. Mean values of PSNR (dB) for different versions of the lost

Fig. (13) and Table 3 show a comparison of the system with and without MDC (SDC). In this method, there is the possibility for image loss. MDC method gives high quality of the image against the loss of versions for the SDC method. Modulation is QPSK, Fading channel, SNR = 15dB, MIMO 2 × 2. PSNR method without using MDC is rarely high.

Fig. 13. Image obtained without MDC

Table 3. PSNR image without MDC

image	PSNR
image cameraman without MDC	28.6540

Fig. (14) illustrates the SNR-PSNR rate of the MDC for the four versions. The result of transmitting DC and next two AC coefficients of the original versions is simulated. In this state, the number of

transmitter antenna 2, the number of receive antenna is 2 (MIMO 2×2), and also the number of transmitter antenna 2, the number of receive antenna is 1, MIMO (2×1) that simulate that is shown in Fig.(14).

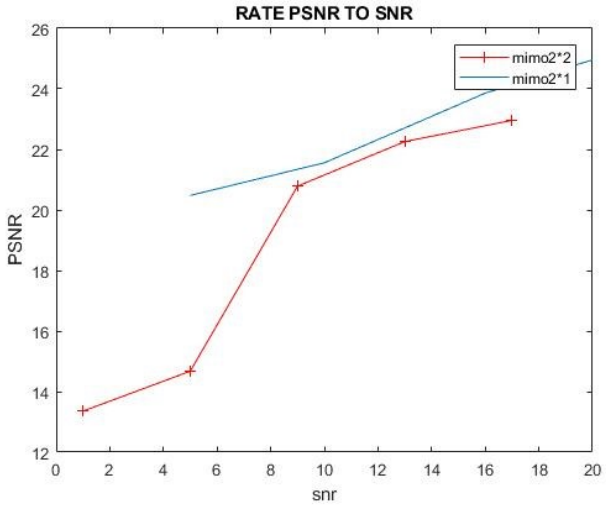

Fig. 14. PSNR than SNR of MDC method with DCT

Table 4 presents the PSNR in the image OSTBC MIMO system using the MDC with four received copies to the dimensions of 128 × 128, Fading channel and SNR = 5,10,15 dB and MIMO 2 × 1 and Spread signals. In this case, the DC has 1 coefficient and AC side has two coefficients of original copies, which have been received with combination of the received four copies obtained by an image in the size of 256 × 256.

TABLE 4. PSNR IMAGE MIMO 2*1

image	**PSNR**
image cameraman	23.8765

Fig. 15. illustrates the SNR Fading channel versus the BER (error rate) of 12 signals (3 coefficients of four copies that are 12) obtained before modulate and after demodulate is drawn.

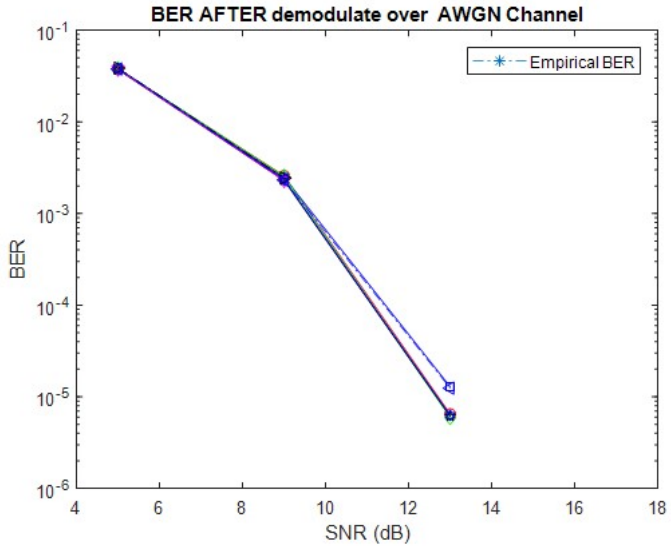

Fig. 15. Error rates after Demodulate

In Fig. (16), the error rate before channel coding and after that have been shown for 12 signals which are set to zero. Therefore, the channel code is used to correct all errors.

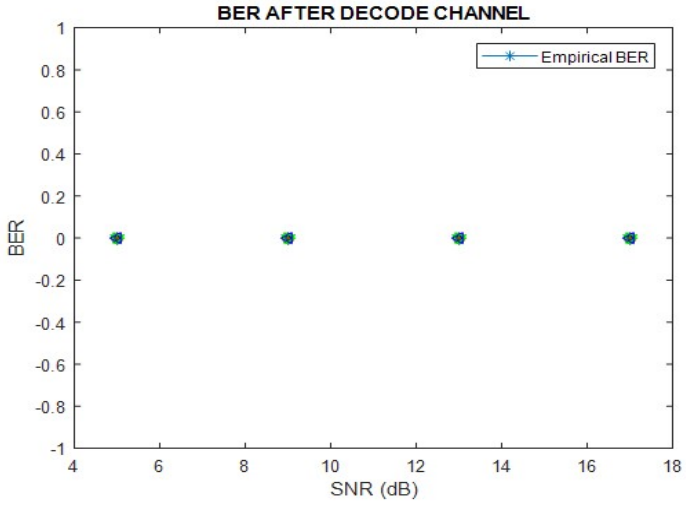

Fig. 16. The error rates after channel decoder

VI. DISCUSSION AND FUTURE TRENDS

UWB facilitates the smooth usage of UAVs in large-scale UAV-CPS applications by extending ultra-wideband localisation with monocular SLAM. Hence, UAV indoor navigation becomes viable in zones without wireless localisation. Furthermore, UWB has scalability repercussions regarding performance. That may help co-operative SLAM involving multiple UAVs, lessening the computational load. UWB can constantly refine the positioning in the presence of sparse reference nodes with a given inertial sensors' structure and particularly tailored for quality assessment of UWB signals [63, 64].

UWB along with a micro Radar system with an Inertial Navigation System (INS), to aid the navigation of small UAV in GNSS-denied situations. UWB and Radar are complementarians where the usage of Radar delivers enough evidence on the present direction while a standalone UWB subsystem may entail a considerable infrastructure to produce adequate location assessments throughout the flight. Velocity from the Radar and positions from the UWB systems can be integrated with an INS, through methodologies like the Extended Kalman Filter (EKF). An Inertial Measurement Unit (IMU) may exhibit a colossal drift owing to the added errors since the can reach several thousands of metres, which calls for an IMU subsystem like GPS, LIDAR, Radar, or UWB to curb inaccuracies. Furthermore, UWB and Radar can be integrated to augment the navigation performance to empower navigation in GNSS-denied settings at a lower cost in terms of infrastructure [65-69].

In communications encompassing compressed video streams is a serious candidate to channel errors degradation. Several approaches exist to mitigate these channel errors. Motion vectors (MVs) interpolation with the support of MV extrapolation (MVE) may conceal corrupted H.264/AVC frames. In UAV-CPSs relying on UWB, the MVs of lost blocks can be recovered or subject to error concealment [49-56] after interpolation with the extrapolated MVs [48-51]. Currently, handling video within UAV-CPSs with the H.264/AVC standard [49] is challenging. Some exciting research like [48] tries to stretch this even more by adopting an H.265 encoder with an adaptive neuro-fuzzy inference system (ANFIS) controller that includes transmission module, control portion and receiver stage with excellent ER and MSE values.

Wireless visual area networks (WVAN) appear everywhere, are stress-free to install and more accessible than various technologies. A WPAN can fit low-speed or high-speed applications. As technology heads towards high-definition videos and other high-end images and video communications, WVAN struggles to deliver quality output. Hence, to unravel this shortcoming, UWB technology is merged with WVAN to

shape the current loopholes, and it results in great quality output with outstanding speed and straightforward access. UWB distinctive features, e.g., high-speed data transmission, low power consumption, inexpensiveness and short-range, make it a choice for delivering high-end imageries and videos in WVAN topology. UWB can be used along with in-loop filtering method to get rid of the blocking artefacts in the output. If computational intelligence is combined with in-loop filtering for classification purposes, then more robustness will be likely achieved with a lesser computational load [50-56, 73, 74, 75].

One of the ultimate challenges for UAVs is a safe landing. From now, visual deployed approaches will become increasingly popular because they are appropriate for landing within the GNSS-denied settings especially when employing ground computing resources for the deployed guidance subsystem and feedbacks the UAV' real-time localisation to its autopilot. A distinct long baseline stereo framework can have an extendable baseline with a wide-angle field of view (FOV) instead of the orthodox fixed-baseline structures under such challenging circumstances. Moreover, theoretical modelling, in addition to computational analysis, assist architectural accuracy evaluations. The UWB positioning network, together with CV-based navigation needs further discussions by the community. Passive UWB anchors along the runway may listen to the UWB signals from UAVs. The ground system can determine the target position contingent to the UWB anchors' geometry and, then, send it back to the UAV.

All forms of wireless channels employed in UAV-CPSs, e.g., RF, optical, acoustical, among others, convey finite resources for remote sensing (RS) with Radar and data communications. Frequently, these two purposes are conflicting, and they contend for common or incompatible resources. WVAN applications are escalating fast, which calls for RF convergence as a prerequisite for all stakeholders to evolve. The ample solution space connected to this multifaceted impasse comprehends collaboration or code signing of CPSs with sensing as well as communications capabilities together. By bearing in mind the UAV-CPSs' needs in unison throughout the design stage, rather than propagating the mutual interference notion, all system's components can have performance enhancements. The UAV-CPS community needs a proper departure design procedure for future enterprises that take into account the applications, topologies, levels of integration, the state of the art while outlining the upcoming data-centric structures [58, 59].

Applications like physical activities, sports, and entertainment demand further studies of UWB moving tags in terms of ranging accuracy and precision. These investigations can confirm some results previously obtained. There is evidence that antenna orientation impacts little the precision of ranging in UWB, while

obstacles influence precision more. Careful UWB parameter tuning and additional new experimental results can impact the precision of the measurements [62].

VII. CONCLUSION

First, this chapter introduces ultra-broadband systems. Next, a hybrid structure based on OSTBC MIMO systems for UAV-CPS image transmission using UWB with QPSK modulation throughout a Rayleigh channels is depicted. Multiple descriptions coding of the image, DCT block of the original image, and how to get the pictures are presented. The MIMO channels examined were the 2 × 2 and 2 × 1 with their respective results compared. Image transmission relying on a number of selected prescription coefficients found by states' spreading with SNR difference, MDC, and SDC. The outcomes showed that at low SNR, the PSNR does not change. Several scenarios for MDC decoding are examined and it was shown that the OSTBC-MIMO system for UAV image transmission is robust. The PSNR is presented with and without MDC. MIMO channel with antenna selection and Alamouti coding. The BER vs SNR curves Alamouti system are simulated. Future work in channel modelling can take into account the increasing the phenomenon of fading with high accuracy.

References

[1] Tractica, "Commercial drone shipments to surpass 2.6 million units annually by 2025," July 2015, pp.

[2] A. K. A. M. amd A. Tuncer, and I. Guvenc, "Unmanned aerial base stations for public safety communications," *IEEE Vehic. Technol. Mag* 2016.

[3] F. C. Commission, "First report and order 02-48," Apr. 2002.

[4] S. G. I. Guvenc, and Z. Sahinoglu, "Ultra-wideband range estimation: Theoretical limits and practical algorithms," *in Proc. IEEE Int. Conf. Ultra-Wideband (ICUWB)* 2008, 3, pp. 93–96.

[5] S. G. I. Guvenc, Z. Sahinoglu, and U. C. Kozat, "Reliable communications for short-range wireless systems," 2011.

[6] X. Lin., "Research of time and frequency synchrinization key technology of frequency hopping in UAV controlling " *[D]UESTC.chengdu,China* 2012.

[7] L. Yunfeng, "Video Coding and Decoding Technology Research Based on Embedded Linux " *[doctoral dissertation]* 2013.

[8] S. R. N. Goddemeier, and C. Wietfeld, "Experimental validation of RSS driven UAV mobility behaviors in IEEE 802.11s networks," *In Globecom Workshops (GC Wkshps), 2012 IEEE* Dec 2012, pp. 1550–1555.

[9] M. H. S. Lupashin, M.W. Mueller, A. P. Schoellig, M. Sherback, and R. D'Andrea, "A platform for aerial robotics research and demonstration " *The flying machine arena. Mechatronics,* 2014.

[10] D. H. S.J. Ingram, and M. Quinlan, "Ultrawideband indoor positioning systems and their use in emergencies," *In Position Location and Navigation Symposium,PLANS 2004*, Apr 2004, pp. 706–715.

[11] L. W. M. Vossiek, P. Gulden, J. Weighardt, and C. Hoffmann, "Wireless local positioning - concepts, solutions, applications. ," *In Radio and Wireless Conference, 2003. RAWCON '03. Proceedings* Aug 2003., pp. 219–224.

[12] M. Z. W. a. R. A. Scholtz, "Impulse radio: how it works,". *Communications Letters, IEEE* Feb 1998, 2, pp. 36–38.

[13] R. A. S. J.M. Cramer, and M.Z. Win, "Spatio-temporal diversity in ultra-wideband radio," *In Wireless Communications and Networking Conference. WCNC. 1999 IEEE* 1999, 2, pp. 888–892.

[14] F. N. a. F. Remondino, “Uav for 3d mapping applications: a review,” *Applied Geomatics* 2014, 6, pp. 1–15.
[15] H. K. Amit Shukla, “Application of robotics in onshore oil and gas industry a review part i,” *Robotics and Autonomous Systems,* 2016, 75, pp. 490 – 507.
[16] C. Z. a. J. M. Kovacs, “The application of small unmanned aerial systems for precision agriculture: a review,” *Precision Agriculture,* 2012, 13, pp. 693–712,.
[17] D. S. J. Qi, H. Shang, N. Wang, C. Hua, C. Wu, X. Qi, and J. Han, “Search and rescue rotary-wing uav and its application to the lushan ms 7.0 earthquake,” *Journal of Field Robotics,* 2016, 33, pp. 290–321.
[18] Y. K. a. I. Nielsen, “A system of uav application in indoor environment,” *Production & Manufacturing Research* 2016, 4, pp. 2–22.
[19] Z. Q. K. Guo, C. Miao, A. H. Zaini, Ch-L. Chen, W. Meng, L. Xie, “Ultra-Wideband-Based Localization for Quadcopter Navigation,” *World Scientific Publishing Company, Unmanned Systems* 2016, 4, pp. 23–34.
[20] J. B. N. Macoir, B. Jooris, B.V. Herbruggen, J. Rossey, J. Hoebeke and E. D. Poorter, “UWB Localization with Battery-Powered Wireless Backbone for Drone-Based Inventory Management,” *Sensors, 19* 2019, 19.
[21] R. P. França, Y. Iano, A. C. B. Monteiro, R. Arthur, V. V. Estrela, S. L. d. L. Assumpção*, et al.*, “Potential Proposal to Improvement of the Data Transmission in Healthcare Systems,” 2019, pp. 161
[22] A. Herrmann, V. V. Estrela, and H. J. Loschi, “Some Thoughts on Transmedia Communication,” OJCST;11(4). doi: 10.13005/ojcst11.04.01
[23] N. Razmjooy, B. S. Mousavi, F. Soleymani, and M. H. Khotbesara, “A computer-aided diagnosis system for malignant melanomas,” *Neural Comput Appl* 2013, 23, pp. 2059-2071.
[24] P. Moallem, N. Razmjooy, and M. Ashourian, “Computer vision-based potato defect detection using neural networks and support vector machine,” *Int. J. Robot. Autom.* 2013, 28, pp. 137-145.
[25] P. Moallem and N. Razmjooy, “Optimal threshold computing in automatic image thresholding using adaptive particle swarm optimization,” *J. Appl. Res. Tech.* 2012, 10, pp. 703-712.
[26] N. Razmjooy, B. S. Mousavi, M. Khalilpour, and H. Hosseini, “Automatic selection and fusion of color spaces for image thresholding,” *Signal Image Video Process.* 2014, 8, pp. 603-614.
[27] H. Z. T. Lv, X. Wang, X.r. Cui, “A Selective Approach to Improve the Performance of UWB Image Transmission System over Indoor Fading Channels,” *6th International Conference on Wireless Communications Networking and Mobile Computing (WiCOM)* 2010, pp.
[28] I. O. a. M.Hamalainen, “UWB Theory and Applications,” 2004, pp. 1-7,.
[29] M. Z. W. a. R. A. Scholtz, “Ultra-wide bandwidth time-hopping spread-spectrum impulse radio for wireless multiple-access communications,” *IEEE Trans. Commun* Apr. 2000., 48, pp. 679-690.
[30] K. K. Z.Bai, “Performance Analysis of Multiuser DS-PAM and TH-PPM UWB Systems in Data and Image Transmission,” *IEEE Conf* 2005, pp.
[31] W. Z. Z.Bai, S.Xu,W.Liu,K.Kwak, “On the Performance of Multiple Access DS-BPAM UWB Systems in Data and Image Transmission,” *IEEE Conf* 2005, pp.
[32] S. M. Alamouti, “A simple transmit diversity technique for wireless communications,” *IEEE J. Select. Areas Commun* Oct. 1998, 16, pp. . 1451–1467.
[33] H. J. V. Tarokh, and A. R. Calderbank, “Space-time block codes from orthogonal designs,” *IEEE Trans. Inf. Theory* July 1999, 45, pp. . 1456–1467.
[34] T. L. X. Li, G. Yue, and C. Yin, “A squaring method to simplify the decoding of orthogonal space-time block codes,” *IEEE Trans. Commun* Oct. 2001, 49, pp. 1700–1703.
[35] H. S. a. J. H. Lee, “Performance analysis of space-time block codes over keyhole Nakagami-,” *IEEE Trans. Veh. Technol* Mar. 2004, 53, pp. 351–362.
[36] A. H. H. Shah, and A. Nosratinia, “Performance of concatenated channel codes and orthogonal space-time block codes,”*,” IEEE Trans. Wireless Commun* June 2006, 5, pp. 1406–1414.
[37] A. M. a. S. Aıssa, “Capacity of space-time block codes in MIMO Rayleigh fading channels with adaptive transmission and estimation errors,” *IEEE Trans. Wireless Commun* Sept. 2005, 4, pp. 2568–2578, .
[38] H. Suzuki, “A statistical model for urban radio propagation,” *IEEE Trans. Commun* July 1997, 25, pp. pp. 673–679, .
[39] D. I. L. M. Matthaiou, and J. S. Thompson, “A MIMO channel model based on the Nakagami-faded spatial eigenmodes,” *IEEE Trans. Ant. Propag* May 2008, 56, pp., pp. 1494–1497,.
[40] M. Nakagami, “The ” *in Statistical Methods in Radio Wave Propagation, W. C. Hoffman Ed* 1960, pp. 3–36.

[41] F. Z. T.Kaiser, and E.Dimitrov, "An Overview of Ultra-Wide-Band Systems With MIMO," *in proc. of IEEE* Feb.2009, 97, pp. .285 – 312 , .
[42] V. Kuhn, "Wireless Communications over MIMO Channels," *Universitat Rostock, Germany* 2006, pp. 17.
[43] A. R. R. Y. Wang, S. Lin, "Multiple description coding for video delivery," *Proceedings of the IEEE* Jan. 2005, 93, pp. .57-70, .
[44] V.S.Somayazulu, "Multiple access performance in UWB systems using time hopping vs. direct sequence spreading," *in Proc. IEEE Wireless Communications and Networking Conf* Mar. 2002, 2, pp. 522-525.
[45] M. N. A. Arshaghi, M. Ashourian, "Image Transmission in MIMO-UWB Systems Using Multiple Description Coding (MDC) Over AWGN and Fading Channels with DS-PAM Modulation," *World Essays Journal* 2017, 5, pp. 12-24.
[46] A.Goldsmith, "Wireless Communications," *Stanford University* 2004, pp. 315-320.
[47] H. Jafarkhani, "Space-Time Coding Theory and Practice," *Cambridge University Press,ISBN: 978–0–511–11562–2*.
[48] S. M. A. Salehizadeh. "Motion and Noise Artifact Detection and Vital Signal Reconstruction in ECG/PPG based Wearable Devices." 2015.
[49] H. Marins, and V. V. Estrela. "On the Use of Motion Vectors for 2D and 3D Error Concealment in H.264/AVC Video." In Feature Detectors and Motion Detection in Video Processing, ed. Nilanjan Dey, Amira Ashour and Prasenjit Kr. Patra, 164-186, 2017. doi:10.4018/978-1-5225-1025-3.ch008
[50] J. Zhou, B. Yan, and H. Gharavi. "Efficient Motion Vector Interpolation for Error Concealment of H.264/AVC." IEEE Transactions on Broadcasting 57 (2011): 75-80.
[51] M.A. de Jesus, and V.V. Estrela. "Optical Flow Estimation Using Total Least Squares Variants." Orient. J. Comp. Sci. and Technol;10(3):2017, 563-579. doi: 10.13005/ojcst/10.03.03
[52] Y. Li, and R. Chen. "Motion vector recovery for video error concealment based on the plane fitting." Multimedia Tools and Applications 76 (2017): 14993-15006.
[53] TL Lin, CJ Wang, TL Ding, GX Huang, WL Tsai, TE Chang, and NC Yang. "Recovery of Lost Color and Depth Frames in Multiview Videos." IEEE Transactions on Image Processing 27 (2018): 5449-5463.
[54] M. Usman, X. He, KM Lam, M. Xu, SMM Bokhari, and J. Chen. "Frame Interpolation for Cloud-Based Mobile Video Streaming." IEEE Transactions on Multimedia 18 (2016): 831-839.
[55] D. Chatzopoulos, C. Bermejo, Z. Huang, and P. Hui. "Mobile Augmented Reality Survey: From Where We Are to Where We Go." IEEE Access 5 (2017): 6917-6950.
[56] YL Chen, H. Wang, Y. Hu, and A Malik. "Intra-Frame Error Concealment Scheme Using 3D Reversible Data Hiding in Mobile Cloud Environment." IEEE Access 6 (2018): 77004-77013.
[57] W. Kong, T. Hu, D. Zhang, L. Shen and J. Zhang. "Localization Framework for Real-Time UAV Autonomous Landing: An On-Ground Deployed Visual Approach." Sensors, 2017.
[58] B. Paul, A. R. Chiriyath, and D. W. Bliss. "Survey of RF Communications and Sensing Convergence Research." IEEE Access 5 (2017): 252-270.
[59] S. C. Surender, R. M. Narayanan, and C. R. Das. ''Performance analysis of communications & radar coexistence in a covert UWB OSA system," in Proc. IEEE Global Telecommun. Conf. (GLOBECOM), 2010. pp. 1–5.
[60] D. Garmatyuk, Y. J. Morton, and X. Mao, ''On co-existence of in-band UWB-OFDM and GPS signals: Tracking performance analysis,'' in Proc. IEEE/ION Position, Location Navigat. Symp., May 2008, pp. 196–202.
[61] CB Barneto, L. Anttila, M. Fleischer, and M. Valkama. "OFDM Radar with LTE Waveform: Processing and
[62] T. Risset, C. Goursaud, X. Brun, K. Marquet, and F. Meyer. "UWB Ranging for Rapid Movements." 2018 International Conference on Indoor Positioning and Indoor Navigation (IPIN) (2018): 1-8.
[63] J. Tiemann, A. Ramsey, and C. Wietfeld. "Enhanced UAV Indoor Navigation through SLAM-Augmented UWB Localization." 2018 IEEE International Conference on Communications Workshops (ICC Workshops) (2018): 1-6.
[64] J. Tiemann, F. Eckermann, and C. Wietfeld. "ATLAS - an open-source TDOA-based ultra-wideband localization system." In 2016 International Conference on Indoor Positioning and Indoor Navigation (IPIN), Alcala de Henares, Madrid, Spain, Oct 2016.
[65] S. Zahran, M, Mostafa-Sami, A. Masiero, A. Moussa, A. Vettore and N. El-Sheimy. "Micro-Radar and UWB Aided UAV Navigation in GNSS Denied Environment." (2018).
[66] C. Cadena, L. Carlone, H. Carrillo, Y. Latif, D. Scaramuzza, J. Neira, J.J., Leonard. "Past, Present, and Future of Simultaneous Localization and Mapping: Toward the Robust Perception Age." IEEE Transactions on Robotics, 32(6), 1309– 1332. 2016.

[67] K. Kauffman, J. Raquet, Y. Morton, and D. Garmatyuk. “Real-Time UWB-OFDM Radar-Based Navigation in Unknown Terrain.” IEEE Transactions on Aerospace and Electronic Systems, 49(3), 1453–1466, 2013.
[68] E. Kim, and D. Choi. A UWB positioning network enabling unmanned aircraft systems auto land. Aerospace Science and Technology, 58, 418-426, 2016.
[69] G. A. Kumar, A. K. Patil, R. Patil, S. S. Park, and Y. H. Chai, 2017. “A LiDAR and IMU Integrated Indoor Navigation System for UAVs and Its Application in Real-Time Pipeline Classification.” Sensors, MDPI, 2017.
[70] H.J. Loschi, V.V. Estrela, O. Saotome, J. Hemanth, W.S. Farfan, RJ Aroma, C. Saravanan, EGH Grata, Emergency Response Cyber-Physical Framework for Landslide Avoidance with Sustainable Electronics. Technologies, 6, 42, 2018. doi:10.3390/technologies6020042.
[71] ACB Monteiro, RP França, VV Estrela, Y Iano, A Khelassi, N. Razmjooy, Health 4.0: Applications, Management, Technologies and Review. Med Tech J, 2(4):262-76, 2019.
[72] TO Edoh. “Smart medicine transportation and medication monitoring system in EPharmacyNet.” 2017 International Rural and Elderly Health Informatics Conference (IREHI) (2017): 1-9. doi: 10.1109/IREEHI.2017.8350381
[73] DJ Hemanth, VV Estrela. Deep Learning for Image Processing Applications, Advances in Parallel Computing Series, Vol. 31, IOS Press, 2017. ISBN 978-1-61499-821-1 (print), ISBN 978-1-61499-822-8 (online)
[74] N Razmjooy, V. V. Estrela, H. J. Loschi, and W. S. Farfan. A Comprehensive Survey of New Meta-heuristic Algorithms. In: Dr. Sourav De, Dr. Sandip Dey and Prof. (Dr.) Siddhartha Bhattacharyya. (eds) Recent Advances in Hybrid Metaheuristics for Data Clustering, 2019.
[75] N Razmjooy, and V. V. Estrela. "Applications of Image Processing and Soft Computing Systems in Agriculture." 1-337, 2019. doi:10.4018/978-1-5225-8027-0
[76] DA do Nascimento, Y Iano, HJ Loschi, N Razmjooy, R Sroufe, V Oliveira, D Castro, and M. Montagner. “Sustainable Adoption of Connected Vehicles in the Brazilian Landscape: Policies, Technical Specifications and Challenges. Transactions on Environment and Electrical Engineering,” 3(1), 44-62, 2019. doi: 10.22149/teee.v3i1.130
[77] N Razmjooy, and M Ramezani. “Using Quantum Gates to design a PID Controller for Nano robots.” Int. Res. J. Appl. Basic Sci. 8, 2354–2359, 2014.